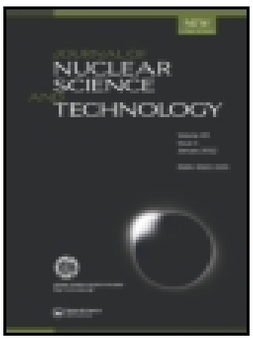

Journal of Nuclear Science and Technology

ISSN: (Print) (Online) Journal homepage: https://www.tandfonline.com/loi/tnst20

New-designed in-situ measurement system for radon concentration in soil air and its application in vertical profile observation

Hao Wang, Lei Zhang, Yunxiang Wang, Changhao Sun & Qiuju Guo

To cite this article: Hao Wang, Lei Zhang, Yunxiang Wang, Changhao Sun & Qiuju Guo (2021): New-designed in-situ measurement system for radon concentration in soil air and its application in vertical profile observation, Journal of Nuclear Science and Technology, DOI: 10.1080/00223131.2021.1961638

To link to this article: https://doi.org/10.1080/00223131.2021.1961638

Published online: 30 Aug 2021.

JOURNAL OF NUCLEAR SCIENCE AND TECHNOLOGY
https://doi.org/10.1080/00223131.2021.1961638

ARTICLE

New-designed in-situ measurement system for radon concentration in soil air and its application in vertical profile observation

Hao Wang[a,b], Lei Zhang[b], Yunxiang Wang[a], Changhao Sun[b,c] and Qiuju Guo[a]

[a]State Key Laboratory of Nuclear Physics and Technology, School of Physics, Peking University, Beijing, China; [b]Solid Dosimetric Detector and Method Laboratory, State Key Laboratory of NBC Protection for Civilian, Beijing, China; [c]School of Nuclear Science and Technology, University of South China, Hengyang, Hunan, China

ABSTRACT

Radon in soil is a valuable radioactive tracer in earth science, especially for earthquake and volcanic precursors. For the purpose of continuous measurement of radon-in-soil concentration in-situ, a new-designed measurement system was developed. Calibration and experiments for humidity response correction were carried out in details, and field measurement of vertical profile with 7 radon probes at different depths was performed. Calibration results show that the sensitivity of the radon probes is 16.1 ± 1.0 cph (kBq m^{-3})$^{-1}$, and the lower level detection limit is 231 ± 15 Bq m^{-3} for 1-hour measurement cycle under the absolute humidity of 32.8 g m^{-3}. Field measurement results show that radon concentrations at different depths change with time and increase with depth in the soil. The vertical profile presents a negative exponential distribution with different diffusion length in sunny days, while rainfall can disturb the vertical distribution and lead to increase of radon concentration in the near ground surface. Radon concentration in underground deeper than 80 cm appears quite stable and hardly affected by rainfall in our observation.

ARTICLE HISTORY
Received 13 May 2021
Accepted 26 July 2021

KEYWORDS
Radon-in-soil; activity concentration; humidity correction; in-situ measurement; vertical profile

1. Introduction

Radon is a naturally occurring radioactive gas generated by the decay of ^{226}Ra-bearing mineral in soils and rocks. Since radon is an inert gas, it can move freely from the soil or building materials, and escape into the atmosphere or seep into the indoor environment. The natural radiation caused by radon and its short-lived decay products is a major source of the exposure dose received by residents [1]. The radon in the soil subjacent to a house is usually the main source of indoor radon [2]. Thus, measurement of radon-in-soil concentration is essential to reduce radon exposure for the Public. In addition, radon-in-soil is also an important tracer for geological, geophysical, and geochemical studies [3]. Especially for seismology, radon-in-soil is considered as a notable precursor and is used to trace the chemical and physical changes during earthquakes and volcanic events [4,5]. However, the radon activity concentration in soil exhibits significant spatial variations and temporal variations, and continuous measurement of radon-in-soil concentration in situ is required consequently [6,7].

Traditional active measurement methods use pump for sampling and adopt scintillation cell, ionization chamber, or electrostatic chamber for radioactive detection. Their high power consumption and inevitable disturbing on radon-in-soil distribution limit their application for long-period continuous field measurement. However, for the passive integrating measurement such as CR-39 and LR-115 detectors, which cannot catch short-term temporal variation in radon-in-soil [8–10]. In-situ continuous measurement technique based on passive sampling and active measurement with low power consumption was also developed and used to monitor the radon-in-soil concentration in the field, such as Clipperton probe [11], Barasol detector [12,13], and RTM1688-2 probe (Sarad, GmbH, Germany) [14]. However, higher sensitivity and more detailed correction of humidity influence are required.

In China, earthquake disaster is one of the most severe natural disaster. Some soil gases including radon have been used as effective tracers for fault activity and earthquake for many years [15,16]. Field investigation and short-term measurement at nearly 1-m or 3-m depth have been being carried out in seismic stations monthly [17–19], using pump for sampling and active measurement device, such as RAD7 and AlphaGUARD, which have high power consumption (several watts) that can only work for a few hours in the field and are expensive. Recently, following the idea of possible seismic precursor [20], a denser and more intelligent detection system is planning to set up in China, which could realize the real-

CONTACT Lei Zhang swofely@pku.edu.cn Solid Dosimetric Detector and Method Laboratory, State Key Laboratory of NBC Protection for Civilian, Beijing 102205, China

time recording of radon-in-soil concentration in situ and the automatic data transmission.

For this purpose, a new-designed in situ measurement system of radon-in-soil with low power consumption and automatic data transmission function was developed in this study, calibration, and humidity response correction experiments were carried out in detail. Furthermore, not like those instantaneous or integrating measurements which could only give short-term or average radon-in-soil concentration distribution profile [21–24], a long-term continuous measurement was performed in situ with seven detectors at different depths in soil at the same location. Vertical profile of radon-in-soil concentration and its temporal variation were observed and analyzed in this paper.

2. Materials and Methods

2.1. Radon-in-soil measurement system

The new-designed radon-in-soil measurement system constituted a radon probe, a rain sensor, a GPRS (General Packet Radio Service) module, and a solar power supply module, as shown in Figure 1(a). The detection principle of radon probe was based on a combination of passive sampling with gas diffusion, electrostatic collection of radon decay products onto the detector, and alpha spectrometry.

In general, the radon probe was installed inside a PVC cylindrical tube with 1 m length and 75 mm diameter, and it was hung up nearly 5 cm above the bottom. Radon-in-soil concentration and rainfall data were recorded and uploaded to the data center automatically through the GPRS module. The power consumption has been reduced to as low as 33.3 mW after optimization. The power supply system consisted of a 12 V lead-acid battery could keep the probe running for more than three months. Besides, as an option, a solar power supply module was used for long-term field measurement.

The radon probe consisted of a wire screen, a waterproofing membrane, four PTFE filters, a measurement chamber, and an electronic unit, as shown in Figure 1(b). Water vapor can pass the membrane while aqueous water is blocked. Four thickness of 1-μm PTFE filters were used to filter out radon progeny and thoron. The response time of the measurement system (refers to the time it required for the

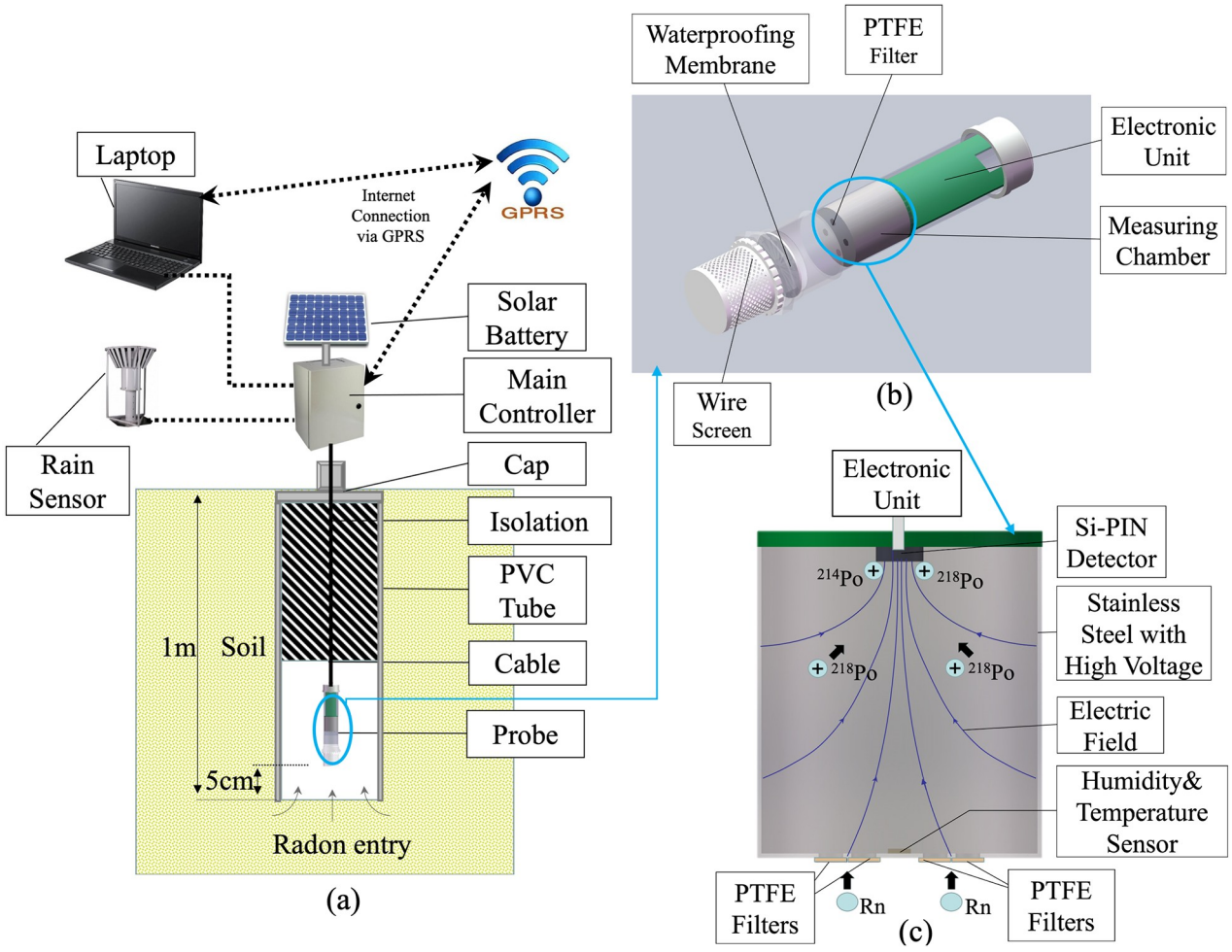

Figure 1. (a) Schematic graph of the radon-in-soil measurement system. (b) Structure chart of the radon probe. (c) Schematic map of the electrostatic collection chamber.

inner radon concentration rising up to as high as outside radon concentration in soil air) was less than 30 min. Multichannel analyzer (MCA) with 256 channels, analog-to-digital converter (ADC), pre- and main-amplifier were integrated in the electronic unit. The structure has been specially designed for the application in water deeper than 3 m.

It is known that thoron (^{220}Rn) exists together with radon in the soil medium. It might be an interference on the accurate radon measurement. Some anti-thoron barriers based on polymer membranes have been developed [25,26]. However, the temperature dependence of radon penetration through the membrane is a notable problem [27]. For our measurement chamber with four 24 mm^2 holes and covered with four specially designed 1 μm × 28 mm^2 PTFE filters, the penetration ratio (the ratio of the concentration inside to outside chamber) of ^{222}Rn was nearly 100% [28,29]. Thus, the temperature influence on the permeability of ^{222}Rn through PTFE was negligible. Although a small amount of ^{220}Rn could penetrate into the chamber, it will be distinguished by the α spectrum detector completely.

The measuring chamber had a volume of 46.4 ml with a 10 mm × 10 mm Si-PIN detector (S3209, Hamamatsu Co, Japan) [30] and a temperature-humidity sensor (SHT31, Sensirion AG, Switzerland) [31] inside. A high voltage of −180 V was loaded on the detector, and the positive ^{218}Po particles originating from radon decay could be collected on the surface of detector due to electrostatic field. The subsequent α decays of ^{218}Po and ^{214}Po could be detected and analyzed by a multi-channel analyzer. According to the principle of electrostatic collection method [32,33] and considering the influence of absolute humidity (i.e. water vapour concentration) on the sensitivity [34], radon concentration was calculated by the following equation:

$$C_{\mathrm{Rn}} = CF(AH_0).\left(\frac{N_1+N_2-0.56N_3}{T}-B\right)\cdot\eta(AH) \quad (1)$$

$$^{\sigma}C_{Rn} = \sqrt{\left(\left(\frac{\sigma_{CF}}{CF}\right)^2+\left(\frac{\sigma_\eta}{\eta}\right)^2\right)\cdot {C_{\mathrm{Rn}}}^2+\left(\frac{N_1+N_2-0.56N_3}{T^2}+B\right)\cdot\eta^2\cdot CF^2} \quad (2)$$

$$\sigma(N_1+N_2-0.56\cdot N_3) = \sqrt{N_1+N_2-0.56\cdot N_3} \quad (3)$$

where C_{Rn} is radon activity concentration (Bq m^{-3}), N_1 is the total counts in the region of interest of ^{218}Po and ^{212}Bi (5.5 ~ 6.2 MeV); N_2, and N_3 are the counts in the region of interest of ^{214}Po (7.0 ~ 7.8 MeV) and ^{212}Po (8.2 ~ 9.0 MeV), respectively. N_3 is used to eliminate the influence of the thoron daughter ^{212}Bi on the measurement of ^{218}Po according to the α decay branch ratio of ^{212}Bi to ^{212}Po, which is 0.56. B is the background counting rate in the region of interest of ^{218}Po and ^{214}Po (cph). T is the measurement cycle (T=1 h). $CF(AH_0)$ is the calibration factor (Bq m^{-3} cph^{-1}) at the reference absolute humidity AH_0. $\eta(AH)$ is the humidity correction coefficient, which is the ratio of sensitivity at absolute humidity AH to that at reference absolute humidity AH_0. $\sigma_{C_{\mathrm{Rn}}}$ is the uncertainty of C_{Rn}, note here that $\sigma_{CF}=0$ as $CF(AH_0)$ is a constant. The uncertainty of the net counts of α particle emitted by ^{214}Po and ^{218}Po ($N_1+N_2-0.56\cdot N_3$) is calculated by Equation(3).

The lower level detection limit (LLD) of radon concentration of the device in 1-hour cycle is calculated by the following equation as defined by Currie (1968) [35] and ISO11929 [36]:

$$C_{\mathrm{DT}} = k\cdot\sigma_{(C_{\mathrm{Rn}}=0)} = k\cdot\sqrt{2M_{\mathrm{B}}}\cdot\eta\cdot CF = k\cdot\sqrt{2M_{\mathrm{B}}}/\varepsilon \quad (4)$$

$$\begin{aligned}\mathrm{LLD} = C_{\mathrm{DT}}+k\cdot\sigma_{(C_{\mathrm{Rn}}=LLD)} &= \frac{2C_{\mathrm{DT}}+k^2/\varepsilon}{1-k^2\cdot{\sigma_\varepsilon}^2/\varepsilon^2}\\ &\approx \left(2.71+4.65\sqrt{M_{\mathrm{B}}}\right)/\varepsilon\end{aligned} \quad (5)$$

where is ε the sensitivity at the reference absolute humidity AH_0, which is equal to $1/CF(AH_0)$ with a dimension of cph (Bq m^{-3})$^{-1}$, and M_B is the total background counts in the region of interest of ^{218}Po and ^{214}Po for 1-hour cycle. C_{DT} is the decision threshold, $k=1.65$ for the confidence level of 95%.

2.2. Calibration and field measurement

Calibration of 10 radon probes was conducted in a temperature-and-humidity-controlled box with an effective volume of 150 L (KOWINTEST, KW-TH, China) [37]. The relative humidity could be adjusted from 10% to 95% with an uncertainty of 2%, and the temperature control range is from −10 °C to 40 °C with an uncertainty of 0.3 °C. The soil gas pumped from 1 m depth in the soil at a flow rate of 2.5 lpm was used as radon source. The radon concentration in the temperature-and-humidity-controlled box was measured by an AlphaGUARD PQ2000 monitor (Saphymo, France) [38], which can be traced back to the National Radon Standard of Metrological Institute of China.

Due to the significant effect of absolute humidity on the sensitivity of the electrostatic collection method [39], calibration was performed at seven different absolute humidity, from 2.01 to 32.8 g m^{-3}. At each absolute humidity, the temperature and relative humidity were kept stable for more than 24 hours. The background of the radon probe, which is mainly from the electronic noise and residual radon attached to the inner wall of the chamber, was determined by putting the devices into a 30-L stainless steel barrel with activated charcoal inside, and the barrel had been flushed with high-purity N_2 for more than 48 hours.

For continuous observing the vertical profile of radon concentration in soil, a long-term field measurement was carried out in a grove in Beijing

(40.24 °N, 116.71 °E). 7 radon probes, a rain sensor, a GPRS module, and one power supply module were used for field measurement. For the measurement, a hole was dug and then seven radon probes successively mounted on a straight iron rod were embedded vertically, from 20 cm to 140 cm in depth with 20 cm spacing. Original soil was backfilled to prevent radon leakage and disturbance. The field measurement was carried out from 11 July to 26 August 2020, with radon-in-soil concentration and rainfall data recorded hourly.

3. Results and Discussion

3.1. The sensitivity and low-level detection limit

Soil temperature and humidity vary in a large range in field environment. Considering the fact that the radon electrostatic detector is influenced by humidity, the sensitivity of radon probes was calibrated in a rather large range of absolute humidity in this paper. The sensitivity calibration results of 10 probes at different absolute humidity are shown in Table 1.

Results show that the sensitivity of almost all radon probes went down with the increasing of absolute humidity. The sensitivity of the 10 radon probes was slightly different at the same humidity. At 32.8 g/m^3, the maximum and minimum values of the sensitivity of all probes were 14.7 cph (kBq m^{-3})$^{-1}$ and 17.9 cph (kBq m^{-3})$^{-1}$, with a relative deviation of nearly 20%. Took 32.8 g/m^3 as reference absolute humidity AH_0, the average sensitivity of all radon probes was 16.1 ± 1.0 cph (kBq m^{-3})$^{-1}$. The average background was 0.044 ± 0.016 cph, and the low-level detection limit was 231 ± 15 Bq m^{-3} for 1-hour cycle.

The formulae for calculating the uncertainty of average sensitivity used in our paper are as follows:

$$\sigma_{\bar{\varepsilon}} = \sqrt{\frac{\sum_{i=1}^{10} (\varepsilon_i - \bar{\varepsilon})^2}{10 \times (10-1)}} \tag{6}$$

$$\sigma_s = \frac{\sum_{i=1}^{10} \sigma_{\varepsilon_i}}{10} \tag{7}$$

$$\sigma = \sqrt{\sigma_{\bar{\varepsilon}}^2 + \sigma_s^2} \tag{8}$$

where $\sigma_{\bar{\varepsilon}}$ is standard deviation of the averages, σ_s is systematical error of the device, σ is the uncertainty of the averages.

As the radon activity concentration in soil usually ranges from several kBq m^{-3} to tens of kBq m^{-3}, the counts registered per hour were usually higher than 100 even in extremely high absolute humidity. Therefore, for radon-in-soil measurement, the uncertainty caused by the statistical fluctuation is low.

3.2. The humidity correction coefficient

In an attempt to obtain the correction coefficient $\eta(AH)$ at different humidity, the relationship between sensitivity and absolute humidity should be established. Considering that the correlation of different radon probes is a little different, calculation should be performed for each probe, respectively. Taking NO.3 and NO.8 radon probes as examples, the sensitivity declined with the increasing of absolute humidity. It exhibited a noticeable negative exponent relationship. So, it could be fitted by a negative exponential function $Y = A + Be^{-CX}$, just as other researchers did [34,40]. The fitting results are shown in Figure 2, with a correlation coefficient R^2 of 0.967 for No.3 and 0.996 for No.8 radon probes, respectively. We assumed that the uncertainty of η(AH) should be smaller than that of sensitivity, which was less than 6%, as η(AH) was obtained by fitting 7 points in Figure 2.

It should be noted that even though the measurement chamber was as small as 46.4 ml, a remarkable decrease of sensitivity along with absolute humidity increase was observed. When soil temperature changed from 30 °C to −10 °C while the relative humidity keeping at nearly 100%, the sensitivity of the radon probe increased by nearly 260%. This effect is worthy to pay close attention.

Table 1. Calibration results of sensitivity at different absolute humidity.

AH(g m^{-3})	2.01	3.53	12.6	14.7	18.5	25.2	32.8
(T(°C), RH(%))	(19.9, 11.7)	(24.5, 15.8)	(25.4, 53.8)	(28.7, 52.3)	(25.1, 80.1)	(30.2, 82.3)	(33.2, 91.3)
Probe number	Sensitivity(cph (kBq m^{-3})$^{-1}$)						
1	64.5 ± 3.4	63.4 ± 3.4	39.6 ± 2.1	35.2 ± 1.9	23.8 ± 1.3	18.2 ± 1.0	15.9 ± 0.9
2	46.3 ± 2.4	43.1 ± 2.4	22.8 ± 1.2	21.8 ± 1.2	21.8 ± 1.2	18.5 ± 1.0	17.9 ± 1.0
3	64.1 ± 3.4	62.9 ± 3.4	39.5 ± 2.1	35.4 ± 1.9	24.2 ± 1.3	19.6 ± 1.0	17.7 ± 0.9
4	67.8 ± 3.5	68.9 ± 3.7	48.9 ± 2.6	42.6 ± 2.3	29.9 ± 1.6	20.8 ± 1.1	16.9 ± 0.9
5	60.3 ± 3.2	61.1 ± 3.3	29.0 ± 1.5	29.5 ± 1.6	20.3 ± 1.1	16.7 ± 0.9	14.7 ± 0.8
6	66.5 ± 3.5	64.2 ± 3.5	40.0 ± 2.1	36.1 ± 1.9	24.9 ± 1.3	18.1 ± 1.0	15.3 ± 0.8
7	62.2 ± 3.3	60.9 ± 3.3	35.6 ± 1.9	30.9 ± 1.7	22.2 ± 1.2	17.2 ± 0.9	15.4 ± 0.8
8	59.2 ± 3.1	56.6 ± 3.1	29.1 ± 1.5	27.1 ± 1.5	21.8 ± 1.2	18.0 ± 1.0	14.9 ± 0.8
9	56.9 ± 3.0	53.3 ± 2.9	30.1 ± 1.6	28.5 ± 1.5	23.2 ± 1.2	19.4 ± 1.0	15.5 ± 0.8
10	56.1 ± 2.9	57.8 ± 3.1	28.6 ± 1.5	26.7 ± 1.4	21.4 ± 1.1	18.1 ± 1.0	16.6 ± 0.9
Average	60.4 ± 3.9	59.2 ± 4.0	34.3 ± 3.1	31.4 ± 2.6	23.3 ± 1.5	18.5 ± 1.1	16.1 ± 1.0

3.3. Intercomparison

After the humidity response correction, radon-in-soil concentration measurement could be realized in a wide range environment. To verify the feasibility of humidity response correction and validate the accuracy of the continuous measurement results of the system, an intercomparison of 7 detectors and AlphaGUARD were carried out at three different absolute humidity, the intercomparison results of NO.3 and NO.8 radon probes are shown in Figure 3.

Intercomparison results show that, under three different absolute humidity, the average relative deviation $(\overline{C_{Rn}} - \overline{C_{Rn,AG}})/\overline{C_{Rn,AG}}$ of measurement results between NO.3 radon probe and AlphaGUARD were 2.7%, 0.4%, and −3.0% with uncertainty of 7.1%, 7.4%, and 8.1%, respectively; for NO.8 radon probe, the average relative deviation were −0.2%, −0.7%, and −3.8% with uncertainty of 7.3%, 7.8%, and 8.3%, respectively. For the rest five probes, whose results were omitted here for conciseness, their average relative deviation under three different absolute humidity were all within ±5% with uncertainty <less than 9%. <These results indicate the reliability and practicability of the humidity response correction.

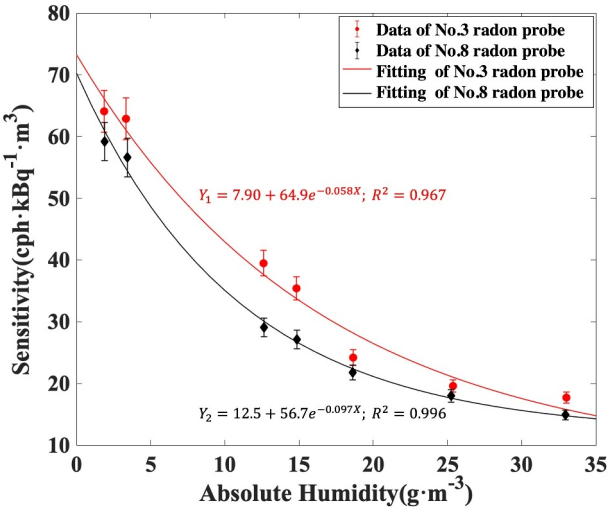

Figure 2. The sensitivity of No.3 and No.8 radon probe at different absolute humidity.

3.4. The temporal variation of vertical profile

The field measurement result from 11 July to 26 August 2020 is shown in Figure 4. The radon concentrations at different depths and rainfall data are presented in upper half of Figure 4. Since the relative humidity at all depths was nearly 100%, only the temperature variations at different depths are shown inlower half of Figure 4.

Results show that the temperature and its variation were quite different at different depths. Soil temperature decreased slightly with the increasing of soil depth in the season of summer and autumn in Beijing. The temperature of near surface in soil showed a distinct diurnal pattern variation, especially at the depth of 20 cm. The temperature fluctuation range in one day could be 2.0 °C to 5.5 °C.

The soil radon concentrations at different depths also changed with time, it increased with the depth on the whole. The soil radon concentration was strikingly affected by the rainfall. After rainfall, the radon concentration in the near surface, such as 20 cm and 40 cm, increased steeply. But no significant change was observed in the deeper soil (120 cm and 140 cm). Taking the data from 31 July to 3 August and from 12 August to 14 August as examples, the radon concentration at 20 cm depth increased 2.9 times and 2.3 times within one day after rainfall, respectively. While the radon concentration at 140 cm only increased 1.22 times and 1.18 times, respectively. In days without rainfall, for instance between 21 July and 26 July, the diurnal variation of radon concentration was observed at

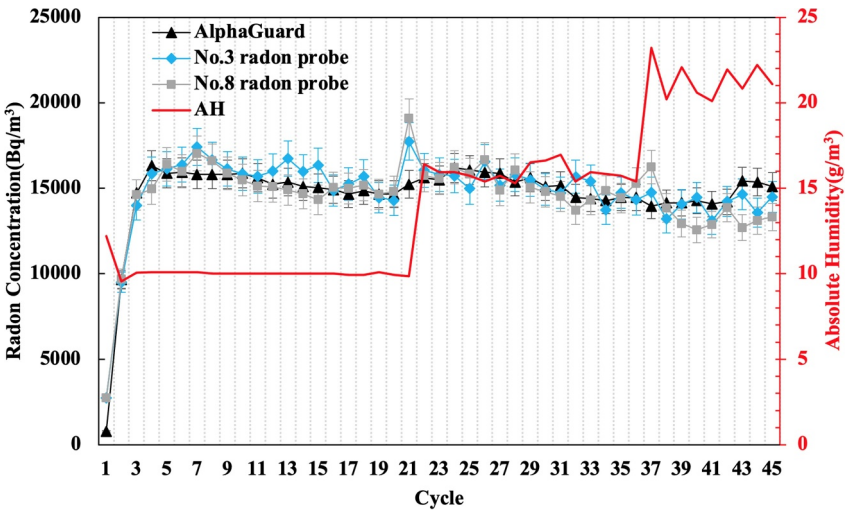

Figure 3. Intercomparison results of AlphaGuard, No.3 and No.8 radon probe at three different absolute humidity.

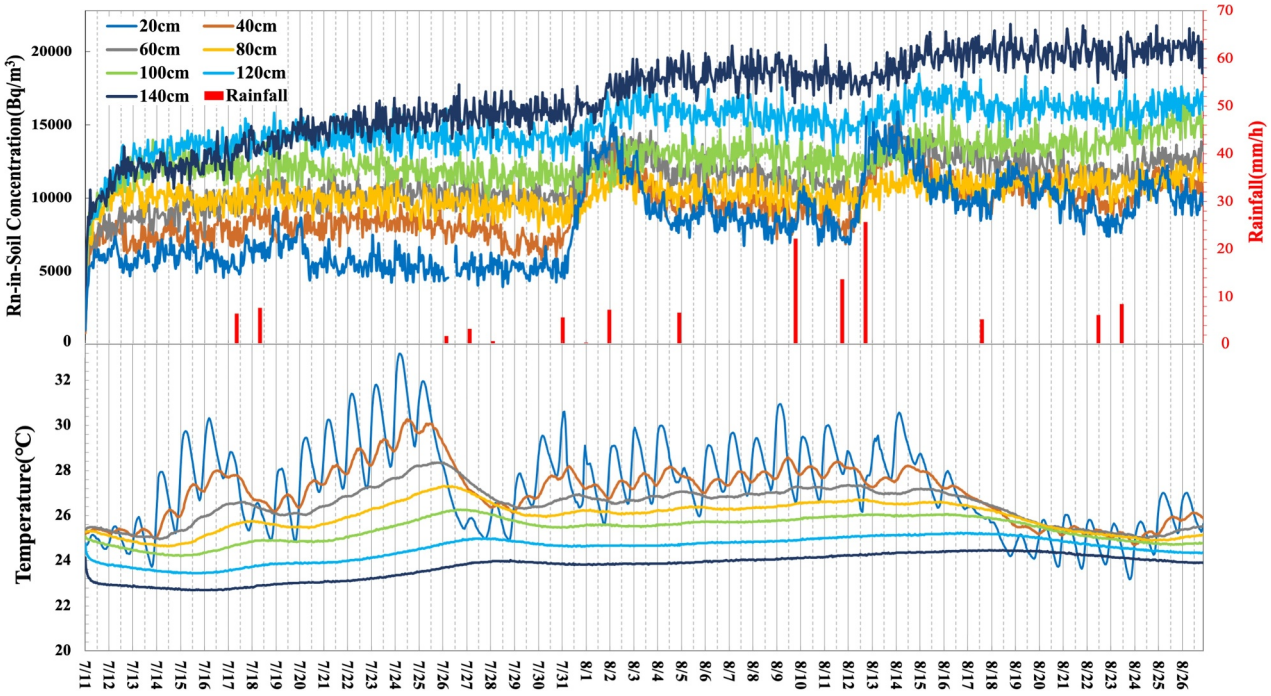

Figure 4. Field measurement result of radon-in-soil concentration and temperature at different depths in 2020.

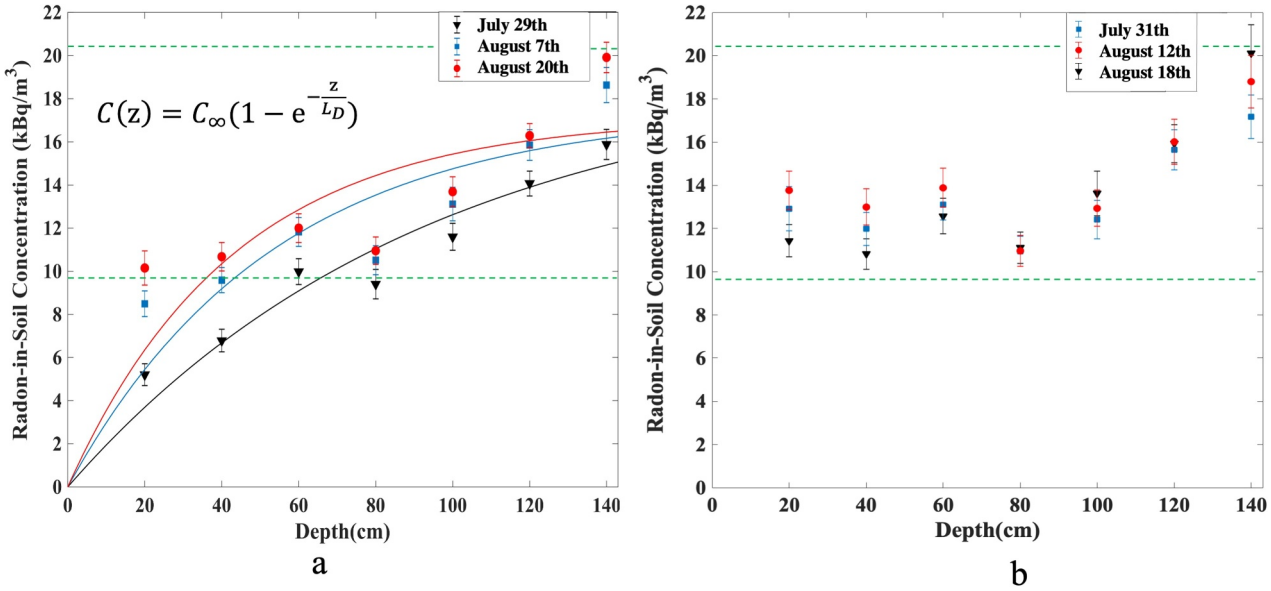

Figure 5. Vertical profiles of radon-in-soil concentration of three periods of sunny days(a) and rainy days(b).

20 cm depth. But this phenomenon was not so obvious in deeper soil.

From Figure 5, it is recognized that the radon-in-soil concentration at each depth had a tendency of slight increase and it rose up considerably and rapidly after sustained rainfall, which might result from the emanation fraction increase caused by the increasing of soil moisture as well as the decreasing of diffusion coefficient [21,41, 42]. Comparing the increasing of soil radon concentration at 20 cm with the rainfall intensity, there seems to be no strong relationship between them. The main reason is that rainfall affects not only the emanation process but also the diffusion process in soil especially near surface [43,44].

It also could be found that the vertical distribution of radon-in-soil is not invariable. To further analyze the vertical distribution, the average radon concentrations at different depths on three sunny (at least 2 days after the end of rainfall) days and three rainy (within 24 h after the rainfall) days are displayed in Figure 5. The selected sunny days were 29 July, 7 August, and 20 August. The selected rainy days were 31 July, 12 August, and 18 August.

In sunny days, radon-in-soil concentration grew up with the increasing of depth, from 5.2 ~ 10.2 kBq m^{-3}

at 20 cm to 15.9 ~ 19.9 kBq m^{-3} at 140 cm. While on rainy days, the radon-in-soil concentrations near the soil surface increased dramatically, which may be due to the sharp reduction in diffusion coefficient. As a consequence, the radon concentration discrepancy at different soil depth shrank immensely. Besides, the difference of radon concentration at >80 cm depth between sunny and rainy day was imperceptible, which might be useful for radon-in-soil survey technical planning.

The experimental points on the three sunny days were fitted using a saturation exponential form of function:

$$C(z) = C_{\infty}\left(1 - e^{-\frac{z}{L_D}}\right) \quad (9)$$

Which has been performed in former papers [23,45]. $C(z)$ is the radon concentration at depth z, and the saturation concentration C_{∞} as well as diffusion length L_D could be obtained through fitting.

C_{∞} was 19.3 kBq m^{-3}, 17.4 kBq m^{-3} and 17.1 kBq m^{-3}, and the corresponding diffusion length L_D was 0.94 m, 0.53 m and 0.43 m, for 29 July, 7 August, and 20 August, respectively. C_{∞} has changed slightly while L_D fluctuated dramatically in different days, which means the diffusion length varies in a large range. It is noteworthy that, the diffusion length L_D in July 29th was 0.94 m, which is larger than the recommended sampling depth of 0.6 ~ 0.8 m by Chinese Standard GB50325-2020 and is close to the sampling depth of 1 m by ISO 11,665–11 [8] for field measurement.

4. Conclusions

For the purpose of continuous monitoring on radon-in-soil activity concentration in field, a new-designed measurement system was developed, and calibration for absolute humidity, intercomparison with alphaGUARD radon monitor as well as a long term field measurement were conducted. Calibration results show that the sensitivity of radon probe changed from 60.4 cph (kBq $m^{-3})^{-1}$ to 16.1 cph (kBq $m^{-3})^{-1}$ as absolute humidity grew up from 2.01 g m^{-3} to 32.8 g m^{-3}, and it appeared an obvious negative exponent relationship. The average sensitivity of the radon probes was 16.1 cph (kBq $m^{-3})^{-1}$ and the lower level detection limit was 231 ± 15 Bq m^{-3} for 1-hour cycle under the reference absolute humidity 32.8 g m^{-3}. Compared with traditional instruments, the measurement system has completely eliminated the influence of humidity. Intercomparison in a large range of absolute humidity was carried out. The relative deviation was within ±5% with uncertainty <less than 9%, Field measurement results show that the radon-in-soil concentrations at different depths changed with time and increased with depth. The vertical profile was not invariable and showed a different distribution in sunny and rainy days, as the radon concentration rose up rapidly in near surface after rain. During sunny days, the vertical profile might also be different with a large variety of the diffusion length.

Long-term online monitoring of radon-in-soil concentration has already been realized in some seismic stations in China. More interesting results will be obtained in the future. In addition, faster response and more accurate measurement on radon-in-soil concentration is still required in the future.

Disclosure statement

No potential conflict of interest was reported by the author(s).

Funding

This work was supported by the National Natural Science Foundation of China [No. 11975310].

References

[1] United Nations Scientific Committee on the Effects of Atomic Radiation. UNSCEAR 2019 Report: sources, Effects And Risks Of Ionizing Radiation. 2019.
[2] International Commission on Radiation Units and Measurements. ICRU. Report 88: measurement and Reporting of Radon Exposures. J ICRU. 2012;12 (2):21-22.
[3] Baskaran M. Radon: a tracer for geological, geophysical and geochemical studies. Switzerland: Springer Nature; 2016. p. 189–226.
[4] Neri M, Ferrera E, Giammanco S, et al. Soil radon measurements as a potential tracer of tectonic and volcanic activity. Sci Rep. 2016;6(1):1–12.
[5] Galli G, Cannelli V, Nardi A, et al. Implementing soil radon detectors for long term continuous monitoring. Appl Radiat Isot. 2019;153:108813.
[6] Hutter AR. Spatial and temporal variations of soil gas 220Rn and 222Rn at two sites in new jersey. Environ Int. 1997;22:455–469.
[7] Winkler R, Ruckerbauer F, Bunzl K, et al. Radon concentration in soil gas: a comparison of the variability resulting from different methods, spatial heterogeneity and seasonal fluctuations. Sci Total Environ. 2001;272(1–3):273–282.
[8] International Organization for Standardization. Measurement of Radioactivity in the Environment—Air: radon 222: part 11: test method for soil gas with sampling at depth. 2016; ISO 11665–11.
[9] George AC. An overview of instrumentation for measuring environmental radon and radon progeny. IEEE Trans Nucl Sci. 1990;37(2):892–901.
[10] Papastefanou C. An overview of instrumentantion for measuring radon in soil gas and groundwaters. J Environ Radioact. 2002;63(3):271–283.
[11] Seidel J, Monnin M. An automatic radon probe for Earth science studies. J Appl Geophys. 1998;39 (4):209–220.
[12] Abbad S, Robe MC, Bernat M, et al. Influence of meteorological and geological parameter variables on the concentration of radon in soil gases: application to

seismic forecasting in the Provence-Alpes-Cote d'Azur region. Environ Geochem Hlth. 1995;16:35–48.
[13] Trique M, Richon P, Perrier F, et al. Radon emanation and electric potential variations associated with transient deformation near reservoir lakes. Nature. 1999;399(6732):137–141.
[14] Sarad G, Germany; 2019 Aug 15 [updated 2020 Mar 27;cited 2021 Jan 5]. Available from: https://sarad.de/
[15] Ying L, Du J, Wang F, et al. Geochemical characteristics of soil gas in the Yanhuai basin, northern China. Earthq Sci. 2009;22(1):93–100.
[16] Zhou X, Du J, Chen Z, et al. Geochemistry of soil gas in the seismic fault zone produced by the wenchuan ms 8.0 earthquake, southwestern china. Geochemical Trans. 2010;11(1):5-5. DOI:10.1186/1467-4866-11-5
[17] Han X, Li Y, Du J, et al. Rn and CO_2 geochemistry of soil gas across the active fault zones in the capital area of China. Nat. Hazards Earth Syst. Sci. 2014;14(10):2803–2815.
[18] Li Y, Du J, Wang X, et al. Spatial Variations of Soil Gas Geochemistry in the Tangshan Area of Northern China. Terr. Atmospheric Ocean. Sci. 2013;24(3):323.
[19] Chen Z, Li Y, Liu Z, et al. Radon emission from soil gases in the active fault zones in the Capital of China and its environmental effects. Sci Rep. 2018;8(1):1–12.
[20] Morales-Simfors N, Wyss RA, Bundschuh J, et al. Recent progress in radon-based monitoring as seismic and volcanic precursor: a critical review. Crit Rev Environ Sci Technol. 2020;3:1–34.
[21] Maeng S, Han SY, Lee SH, et al. Analysis of radon depth profile in soil air after a rainfall by using diffusion model. Nucl Eng Technol. 2019;51(8):2013–2017.
[22] Bem H, Gasiorowski A, Szajerski P, et al. A fast method for the simultaneous determination of soil radon (222Rn) and thoron (220Rn) concentrations by liquid scintillation counting. Sci Total Environ. 2019;709:136127.
[23] Mitev K, Dutsov C, Georgiev S, et al. Unperturbed, high spatial resolution measurement of Radon-222 in soil-gas depth profile. J Environ Radioact. 2018;196(JAN):253–258.
[24] HNP T, Thang NV, Ba VN, et al. Soil radon gas in some soil types in the rainy season in ho chi minh city, vietnam. J Environ Radioact. 2018;193-194:27–35.
[25] Bochicchio F, Ampollini M, Tommasino L, et al. Sensitivity to thoron of an ssntd-based passive radon measuring device: experimental evaluation and implications for radon concentration measurements and risk assessment. Radiat. Meas. 2009;44(9–10):1024–1027.
[26] WJ W, Fleischer RL, Mogro-Campero A. Barrier technique for separate measurement of radon isotopes. Rev Sci Instrum. 1977;48(11):1440–1441.
[27] Fleischer RL, Giard WR, Turner LG. Membrane-based thermal effects in 222Rn dosimetry. Radiat. Meas. 2000;32(4):325–328.
[28] Pressyanov D, Dimitrov D. The problem with temperature dependence of radon diffusion chambers with anti-thoron barrier. Romanian J. Phys.. 2020;65:801.
[29] Bigu J, Hallman ED, Kendrick L Permeability of different materials to radon (222Rn) gas. Sudbury Neutrino Observatory Project Report. 1991; SNO-STR-91-069.
[30] Hamamatsu Photonics Co. 2020 Jan 9 [updated 2020 Aug 9; cited 2020 Nov 11]. Available from: https://www.hamamatsu.com/
[31] Ag S, Switzerland. 2020 Sep 21[updated 2020 Dec 21; cited 2021 Jan 5]. Available from: https://www.sensirion.com/
[32] Wada A, Murayama S, Kondo H, et al. Development of a compact and sensitive electrostatic radon-222 measuring system for use in atmospheric observation. J. Meteorol. Soc. Japan.. 2010;88(2):123–134.
[33] Kiko J. Detector for 222Rn measurements in air at the 1mBq/m3 level. Nucl Instrum Methods Phys Res A. 2001;460(2–3):272–277.
[34] Takeuchi Y, Okumura K, Kajita T, et al. Development of high sensitivity radon detectors. Nucl Instrum Methods Phys Res A. 1999;421(1–2):334–341.
[35] Currie LA. Limits for qualitative detection and quantitative determination. Application to radiochemistry. Anal Chem. 1968;40(3):586–593.
[36] International Organization for Standardization. Determination of the characteristic limits (decision threshold, detection limit and limits of the confidence interval) for measurements of ionizing radiation-Fundamentals and application. 2019; ISO 11929.
[37] Kowintest KW-TH. 2019 Aug 1 [updated 2020 Jan 23; cited 2020 Nov 11]. Available from: http://www.kowintest.cn/
[38] Saphymo, Bertin Instruments. 2017 Dec 17[updated 2021 Aug 8; cited 2020 Sep 16]. Available from: https://www.saphymo.com
[39] Porstendorfer J, Pagelkopf P, Gründel M. Fraction of the positive 218Po and 214Pb clusters in indoor air. Radiat Prot Dosimetry. 2005;113(3):342–351.
[40] De Simone G, Lucchetti C, Galli G, et al. Correcting for H 2 O interference using a RAD7 electrostatic collection-based silicon detector. J Environ Radioact. 2016;162-163(OCT):146–153.
[41] Nazaroff WW. Radon transport from soil to air. Rev Geophys. 1992;30(2):137–160.
[42] Sakoda A, Ishimori Y, Hanamoto K, et al. Experimental and modeling studies of grain size and moisture content effects on radon emanation. Radiat. Meas.. 2010;45(2):204–210.
[43] Rogers VC, Nielson KK. Correlations for predicting air permeabilities and 222Rn diffusion coefficients of soils. Health Phys. 1991;61(2):225–230.
[44] Zhuo, ZHUO W, IIDA T, et al. Modeling Radon Flux Density from the Earth's Surface. J Nucl Sci Technol. 2006;43(4):479–482.
[45] Ryzhakova N. A new method for estimating the coefficients of diffusion and emanation of radon in the soil. J Environ Radioact. 2014;135:63–66.